Supplementary Information

A bifunctional immunosensor based on the Osmium nano-hydrangeas as a catalytic chromogenic and tinctorial signal output for folic acid detection

Junkang Pan[a]; Qiyi He[a,b]; Zhiting Lao[a]; Yikui Zou[a]; Jingyi Su[a]; Qinglan Li[a]; Zekai Chen[a]; Xiping Cui[a,*];Yanfei Cai [c,*]; Suqing Zhao[a,*]

[a] *Department of Pharmaceutical Engineering, School of Biomedical and Pharmaceutical Sciences, Guangdong University of Technology, Guangzhou 510006, People's Republic of China*

[b] *Department of Chemical Engineering and Technology, School of Chemical Engineering and Light Industry, Guangdong University of Technology, Guangzhou 510006, People's Republic of China*

[c] *College of Natural Resources and Environment, South China Agricultural University, Guangzhou510642, People's Republic of China.*

*Corresponding Author:

Dr. Xiping Cui

Tel.: +86 18813758818

E-mail address: cuixiping1989@163.com (X.-P. Cui)

Prof. Yanfei Cai

E-mail address: yanfeicai@scau.edu.cn (Y.-F. Cai)

Prof. Suqing Zhao

Tel.: +86 15820258676

E-mail address: sqzhao@gdut.edu.cn (S.-Q. Zhao)

Chemicals

Folic acid (FA), Tetrahydrofolic acid (THFA), 4-Aminobenzoic acid (PABA), Hydrocortisone (H-CORT), N-(4-aminobenzoyl)-L-glutamic acid (FIGLU), K_2OsCl_6, L-Ascorbic acid (L-AA), glutaraldehyde, was purchased from Macklin Biochemical Co. Ltd. (Shanghai, China). Dihydrofolic acid (DHFA), Pteroic Acid (PA), Methotrexate (MTX), KBr, polyvinylpyrrolidone (PVP, Mw≈10,000), o-Phenylenediamine (OPD), Ovalbumin (OVA), N-(3-(Dimethylamino)propyl)-N'-ethylcarbodiimide hydrochloride (EDC) , $HAuCl_4$ and trisodium citrate were obtained from Aladdin Co. Ltd. (Shanghai, China). Tetramethylbenzidine (TMB)，bovine serum albumin (BSA)，was purchased from Sigma Co. Ltd. (St. Louis, USA). Goat-anti-rabbit IgG and HRP labeled Goat-anti-rabbit IgG was purchased from Bioss Co. Ltd. (Shanghai, China). NC membrane (Sartorius CN140), wicking pad (H5072), adhesive backing (DB-6), sample pad (NJ-Y2) and conjugate pad (Ahlstrom 8964) were obtained from Jieyi Co. Ltd. (Shanghai, China).

PBS (0.01 M, pH 7.4) was prepared by using 8.0 g NaCl, 2.9 g Na_2HPO_4 and 0.2 g NaH_2PO_4 in 1000 mL distilled water. CBS (0.01 M, pH 9.6) was prepared by using 1.5 g Na_2CO_3 and 2.932 g $NaHCO_3$ in 500 mL distilled water. Reconstitution solution contained 5% sucrose, 2% fucose, 1% PEG 20000, 1% BSA and 0.25% Tween-20 in PBS.All the chemicals used in this study were analytical reagent grade. Solutions were prepared with ultrapure water from a Millipore Milli-Q water purification system (Billerica,MA).

Apparatus

The characterization of Matrix-Assisted Laser Desorption/Ionization Time-of-Flight Mass Spectrometer (MALDI-TOF-MS) was measured by Ultraflextreme MALDI-TOF mass spectrometry (Bruker, Germany). Transmission electron microscope (TEM) was conducted with a HT7700 microscope (Hitachi, Japan) and the Scanning electron microscopy (SEM) image was obtained through a Sigma 300 microscope (Zeiss , Germany), Energy dispersive X-ray spectroscopy (EDS) was attended to investigate the elemental analysis for the nanomaterials. X-ray photoelectron spectroscopy (XPS) was performed using Thermo Scientific K-Alpha+ (Thermo Fisher, USA) with Mono AlKα radiation for the analysis of the surface composition and chemical states of the nanomaterials. Zeta potential was determined by Zetasizernano (NanoBrook Omni, USA) to distinguish OsNHs and OsNHs@pAb probe conjugation. The Inductively coupled plasma mass spectrometry (ICP-MS) was presented using ICAP RQ (Thermo Fisher, Germany) to determine the concentration of OsNHs suspension. The ultraviolet spectrogram was measured by Lambda 25 UV/VIS spectrophotometer (PerkinElmer, USA). The UPLC-MS/MS for determining the pre-treated spiked milk powder samples was analysed by Ultimate 3000 liquid phase system and TSQ Endura triple quadrupole mass spectrometer (Thermo Fisher, USA).

Experimental section

Preparation and characterization of antigens

The tailored immunogen (FA-BSA) was certainly made by the glutaraldehyde method with minor modification in order to combine the BSA at the amino site of folic acid[1]. Typically, 18.2 μM of folic acid was dissolved in 4 mL PBS (0.01 M, pH 7.4) before the slow titration in BSA (1.36 μM in 1 mL PBS) at 4℃. Then 30 μL of 50% glutaraldehyde was added into the above solution and reacted at 4°C for 2h in a sheltered environment. Subsequently, 1.5 mL of glycine solution (1M in PBS) was added to stop the reaction and the solution was under multiple ultrafiltration to remove glutaraldehyde and concentrate the volume. The prepared FA-BSA was stored at -20°C before use identified by Sodium dodecyl sulfate-Polyacrylamide gel electrophoresis (SDS-PAGE) and MALDI-TOF-MS.

The coating antigen (FA-OVA) was prepared as the same method mentioned above while used OVA as carrier protein for substitution, which regarded as FA-NH_2-OVA. For further exploration of heterologous effect, the carboxyl group of folic acid was also bonded with OVA to from the heterologous coating antigen (FA-COOH-OVA) using the tool of EDC[2]. Basically, 400 μL of EDC solution (0.078Mm in PBS buffer, pH7.5) was slowly added into 2mL of FA solution (0.01mM in PBS buffer, pH7.5) for 6h activization. Then the reaction solution was centrifuged to obtain the supernatant and added to 200 μL of OVA (0.1μM in PBS buffer, pH7.5). The mixture was stirring at room temperature for 4 h and then in 4°C for 12 h, which was protected from light during the whole reaction. Finally, the prepared FA-COOH-OVA was

obtained after centrifugation and stored at -20°C. Both coating antigens were identified by SDS-PAGE as well.

Preparation of polyclonal antibody (pAb) against FA

Based on the preceding composition[3], Female New Zealand white rabbit was choosen to generate the specificity polyclonal antibodies for folic acid. Briefly, 1 mL FA-BSA (1 $mg \cdot mL^{-1}$) was emulsified with 1 mL Freund's complete adjuvant and injected at multiple sites into the the cervical and retral subcutaneous skin of rabbit. After 14 days of immunological response, the rabbit was infused with an additional 1 mL FA-BSA (1 $mg \cdot mL^{-1}$) emulsified concoction with isometric Freund's incomplete adjuvant to enhance immunisation. The rabbits are subsequently immunised three times every fortnight and their blood are centrifuged to obtain a polyclonal antibody-rich serum. The available serum was collected and stored at -20 ◦C until use. The titer of collected rabbit serum was measured by traditional indirect ELISA.

The Steady-state kinetic experiment

The steady-state kinetic experiment was performed by altering the substrate concentration of TMB and H_2O_2 as follows. Firstly, 50 μL of OsNHs suspension diluted at 100 times with ultrapure water and 50 μL TMB with different concentrations from 0 to 0.8 mM were mixed in 96 well plates followed the addition of 50 μL H_2O_2 (10 mM i) to prompt the reaction for 5 min. Later the absorbance of each sample was immediately measured at 652 nm. Formerly, the preceding experimental procedure was repeated with the invariant concentration of TMB (0.4 mM) and different gradient concentrations of H_2O_2 (0.19, 0.39, 0.78, 1.56, 3.13, 6.25, 12.5 mM) were used. All the

substrate was dispersed in ultrapure water while the TMB was excluded and diluted in in phosphoric-citric acid buffer (0.05M, pH4.0).

The obtained data of the A_{652nm} value were translated to initial reaction rate (υ) using the Lambert-Beer law and calculated by $Slope_{Initial}/(\varepsilon_{oxTMB\text{-}652\ nm} \times l)$, where $\varepsilon_{oxTMB\text{-}652\ nm}$ was molar extinction coefficient of oxTMB at 652 nm. The plots of υ against concentrations of substrate were fitted as nonlinear regression using the Michaelis-Menten equation which is $\upsilon = \upsilon_{max} \times [S]/(K_m + [S])$, where the υ_{max} is maximum reaction, K_m is Michaelis-Menten constant, and [S] is the substrate concentration for TMB or H_2O_2. The apparent steady-state kinetic parameters (K_m and υ_{max}) could be calculated based on the double-reciprocal plots of υ against substrate concentrations (or the Lineweaver-Burk equation). Furthermore, the turnover number K_{cat} can be identified by the equation of $K_{cat} = \upsilon_{max}/[E]$ to explore the peroxidase-like performance for per unit volume concentration, where [E] is the concentration of the nanomaterials (OsNHs) which is available by the ICP-MS.

Preparation of Colloidal Au Nanoparticles.

The 20 nm colloidal AuNPs was prepared according to the dissertation with minor alteration[4]. Briefly, after boiling 100 mL of 0.01% $HAuCl_4$ with 2 mL of 1.0% trisodium citrate in aqueous solution for 15 min stirring, the resulting colloidal suspension was cooled and volumetric to 100ml. To remove the superfluous precipitation, the colloidal solutions was filtered through a 0.45-μm Millipore membrane. The diameter of AuNPs was ~20 nm.

Validation study by UPLC-MS/MS

Aiming to verify results of quantitative analysis by OsNHs-NLISA, with a Hypersil GOLD C18 (10 × 2.1 mm, 1.9 μm, Thermo Scientific), 2 μL of sample solution volume was injected with running time of 7 min. The analysis procedures were examined in Table. S3, which were handled at a flow-rate of 0.3 $mL \cdot min^{-1}$, the mobile phase comprised of solvent A (0.1% Formic acid aqueous solution) and solvent B (Methanol). The gradient profile was as follows: started with 10 % B (hold time 2.0 min); continued with linear change to 90 % B up to 3.0 min; continued 90 % B up to 5.0 min; returned to initial condition at 5.1 min, followed by equilibrium until 7 min. Meanwhile, the temperature of column oven was sustained at 40 ◦C.

On the part of qualitative and quantitative tracking of the FA, atmospheric pressure ionization (APCI) probe operated in positive ion mode was also performed in MS system. Ion source and MS parameters can be seen from Table. S4. Xcalibur software was used for data acquisition and processing in SRM mode. The chromatogram of FA from spiked milk powder samples analyzed by UPLC-MS/MS is shown in Fig. S8.

Results and discussion

Optimization of the experimental parameters of OsNHs–LFIA and AuNPs-LFIA

Aiming to obtain highest sensitivity performance, we conducted serval kinds of parameters to achieve the favorable optimization. To accomplish the desirable optimization, both T- and C-line were contemplated as the identical tinctorial signal. Notably, electrostatic binding effects are essential for the binding of OsNHs and pAb, which can be affected by differing the pH and ionic strength. Here in, we determined

different volume of 0.2M K_2CO_3 and the results (Fig. S5a) indicated that the addition volume of 2 μL·mL^{-1} was considered as the optimal performance while the reduction of activity for antibodies result in blurred lines as the promotion of pH and ionic strength. In addition, the increase in the amount of antibody and OsNHs used also has a significant effect on the tinctorial signal of the test strip lines. As shown in Fig. S5b-c, 5 μL·mL^{-1} of pAb against FA can performed the sufficient tinctorial signal for T-line as well as fewer amount of antibodies always lead to lower detection limits, while 0.5 mL·mL^{-1} of the additional volume was suitable for the detection mode and saved the usage of OsNHs. Furthermore, the better achievement of the lower detection limits was seriously related to the concentration of coating antigen represented by the T-line in the indirect competitive detection mode. It can be obviously seen at Fig. S5d that as the concentration of coating antigens reached to 0.5 mg·mL^{-1} the T-line signal was strong enough. Besides, the exaggerated amount coating antigens can cause the T-line to become deeper, resulting in redundant OsNHs@pAb probe binding to the T resulting in reduced sensitivity of the assay.

Similarly, the AuNPs-LFIA was conducted as the same optimization to perform a gratifying sensitivity performance as OsNHs–LFIA. As shown in Fig. S6, 2 μL of K_2CO_3 and 20 μL·mL^{-1} pAb are the optimal parameter for AuNPs-LFIA. Besides, these two parameters of volume of the nanomaterials and T-line concentration are optimised to be consistent with OsNHs–LFIA. After all the experimental parameters were defined, a serious of sensitivity experiment was executed by an indirect competitive detection mode for both OsNHs–LFIA and AuNPs-LFIA, which appraised as distinction.

Figure and table captions

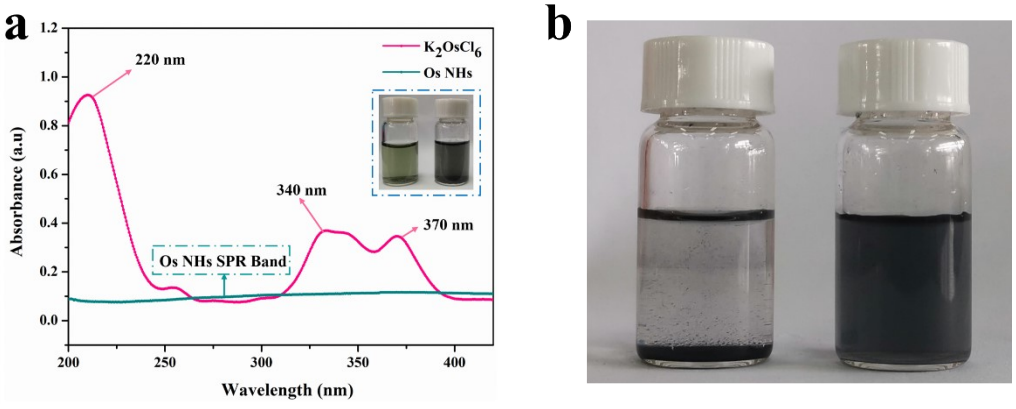

Fig. S1 (a) Typical absorbance spectra between K_2OsCl_6 and OsNHs (inset shows the photograph of bare K_2OsCl_6 and OsNHs solutions); **(b)**Photographs of suspensions of ordinary OsNPs (left) stored at room temperature for 30 days and OsNHs (right) stored at room temperature for 30 days.

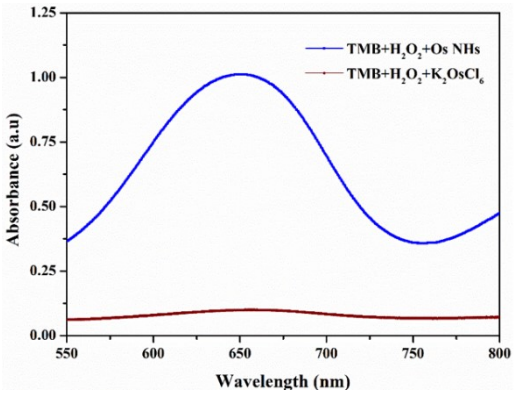

Fig. S2 The UV-Vis spectrogram of OsNHs(Os^0)+TMB+H_2O_2 (blue line) and K_2OsCl_6(Os^{4+})+TMB+H_2O_2 (wine line). In detail: 300 μL of TMB (0.4mM in Phosphoric-citric acid buffer, 0.05M, pH4.0), 600 μL of H_2O_2 (10mM in water), and 300 μL of OsNHs or K_2OsCl_6 dispersion (diluted 500 times in ultrapure water) was added to mixture for 5 min. Finally, the mixture was allowed to the spectral studies

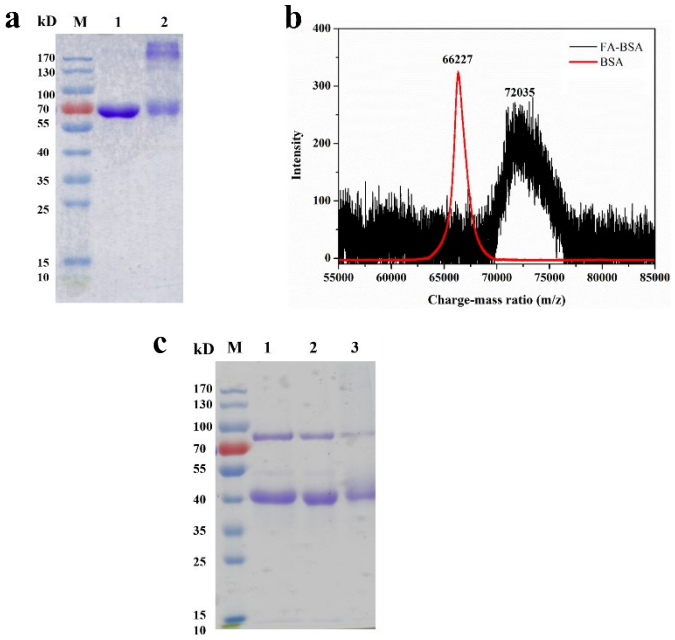

191

192 **Fig. S3** Characterization of prepared immunogen and coating antigen. **(a)** SDS-PAGE
193 characterization of FA immunogen: strip1, BSA; strip2, FA-BSA; **(b)** MALDI-TOF-
194 MS characterization of FA-BSA (black line) and BSA (red line). **(c)** Characterization
195 of coating antigen. SDS-PAGE characterization of FA coating antigens: strip1, FA-
196 COOH-BSA; strip2, OVA; strip3, FA-NH_2-OVA.

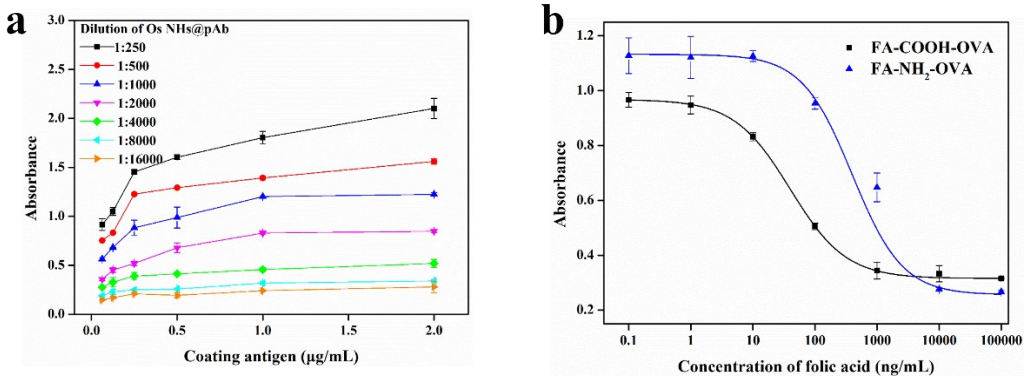

197

198 **Fig. S4** Optimization results of the experimental parameters of OsNHs-NLISA
199 immunosensor. **(a)** The chessboard results of OsNHs-ELISA; **(b)** Standard curve
200 against FA-COOH-OVA and FA-NH_2-OVA for the homologous and heterologous
201 effect study.

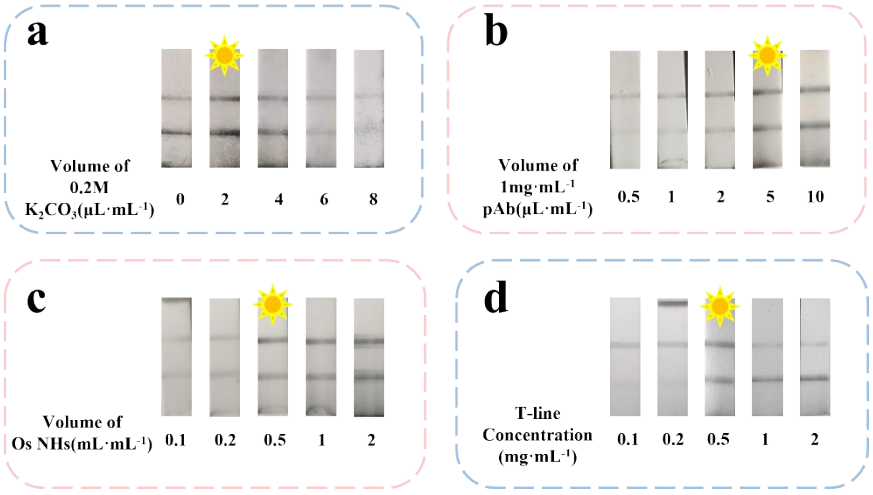

202

203 **Fig. S5** Optimization results of experimental parameters of the OsNHs-LFIA
204 immunosensor. The volume selection of 0.2 M K_2CO_3 (μL) performed in OsNHs-LFIA
205 **(a)**; The volume selection of 1mg·mL^{-1} anti-FA pAb (μL) performed in OsNHs-LFIA
206 **(b)**; The additional volume selection of OsNHs (mL) performed in OsNHs-LFIA **(c)**,
207 which the final volume of the mixture is determined at 1 mL; The volume selection of
208 T-line concentration (mg·mL^{-1}) performed in OsNHs-LFIA **(d)**.

209

210

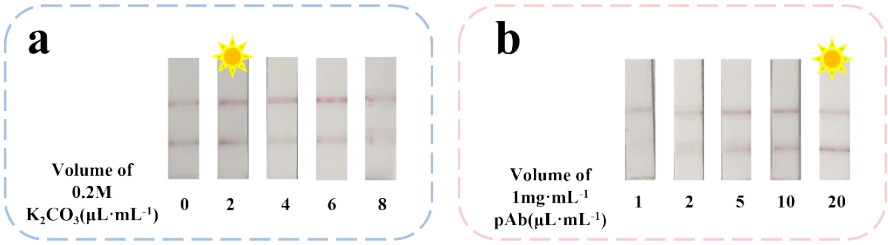

211

212 **Fig. S6** Optimization results of experimental parameters of the AuNPs-LFIA. The
213 volume selection of 0.2 M K_2CO_3 (μL) performed in GNPs-LFIA **(a)**, The volume
214 selection of 1mg·mL^{-1} anti-FA pAb (μL) performed in GNPs-LFIA **(b)**.

215

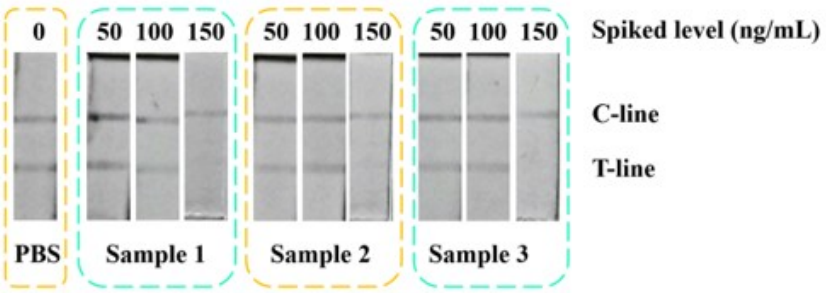

Fig. S7 Recovery of FA from spiked milk powder samples by OsNHs-LFIA for qualitative detection. All experiments were performed in triplicate.

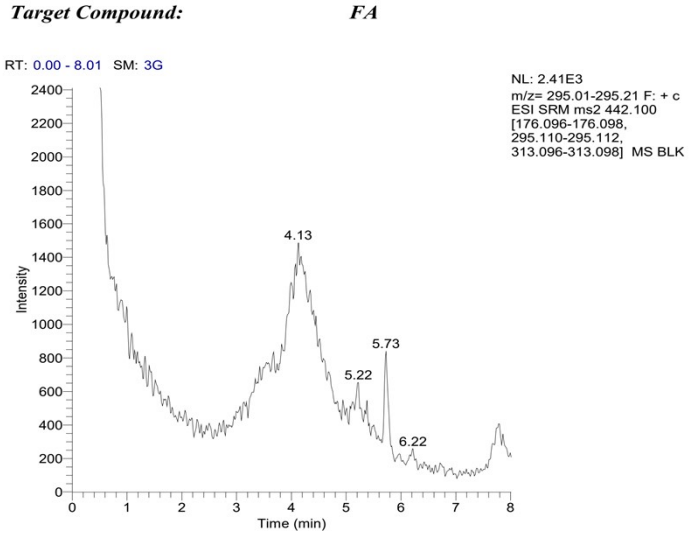

Fig. S8 The chromatogram of FA from spiked milk powder samples analyzed by UPLC-MS/MS.

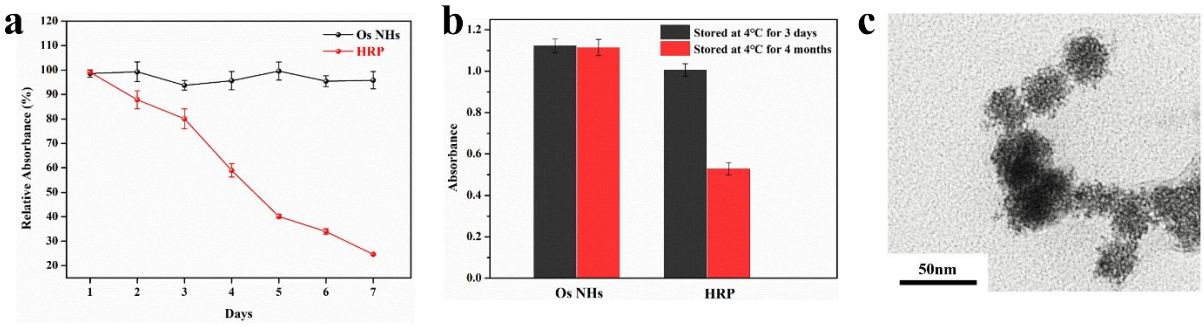

Fig. S9.A short and long-time storage stability study between OsNHs and HRP. **(a)** Storage stability for 7 days at room temperature and **(b)** storage stability compared between 3 days and 4 months at 4℃. **(c)** TEM image of OsNHs taken after four months of storage at 4℃.

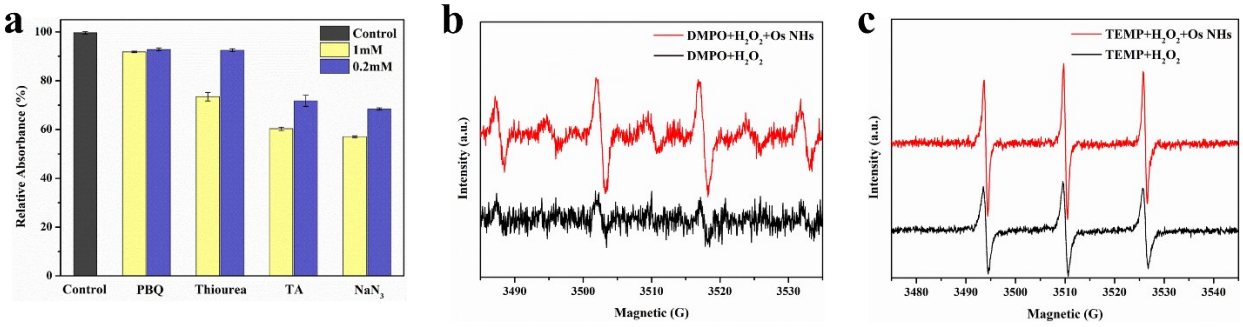

Fig. S10.The study of mechanisms of peroxidase-like activity for OsNHs. (a) The relative absorbance of OsNHs-TMB-H_2O_2 catalytic system with or without ROS scavengers at 450nm. (b) ESR spectra of the formation of ·OH trapped by DMPO in the OsNHs-H_2O_2 catalytic system. (c) ESR spectra of the formation of $^1O_2$ trapped by TEMP in the OsNHs-H_2O_2 catalytic system.

244 **Table S1** Apparent steady-state kinetic parameters for OsNHs and other metallic NPs

245 peroxidase mimic

Enzyme or Enzyme mimic	Substrate	K_m (mM)	υ_{max} ($10^{-8}Ms^{-1}$)	[S] (M)	K_{cat} (s^{-1})	K_{cat}/K_m ($s^{-1}mM^{-1}$)	Ref.
HRP	TMB	0.434	10	2.5×10^{-11}	4.0×10^{3}	9.2×10^{3}	5
	H_2O_2	3.7	8.71		3.48×10^{3}	0.94×10^{3}	
Fe_3O_4NPs	TMB	0.098	3.44	1.14×10^{-12}	3.02×10^{4}	3.08×10^{5}	5
	H_2O_2	154	9.78		8.58×10^{3}	5.6×10^{2}	
Co_3O_4NPs	TMB	0.037	6.3	3.4×10^{-10}	1.8×10^{3}	4.86×10^{5}	6
	H_2O_2	140	12		3.5×10^{3}	25	
PtNPs	TMB	0.12	130	8.1×10^{-11}	2.3×10^{4}	1.92×10^{6}	7
	H_2O_2	770	190		1.6×10^{4}	20.78	
Cit-IrNPs	TMB	0.91	170	3.4×10^{-7}	0.5×10^{3}	5.5×10^{3}	8
	H_2O_2	0.27	150		0.44×10^{3}	1.6×10^{3}	
RhNPs	TMB	0.20	6.78	1.75×10^{-10}	0.39×10^{3}	1.95×10^{3}	9
	H_2O_2	0.38	24.1		1.38×10^{3}	3.63×10^{3}	
Pt_{10}-LP NCs	TMB	0.265	50.3	N/A	N/A	N/A	10
	H_2O_2	2.64	10.2				
Bare-Pd	TMB	1.04	11.4	N/A	2.2×10^{-3}	2.1×10^{5}	11
	H_2O_2	6.60	24.8		4.8×10^{-3}	7.2×10^{4}	
His-Pd	TMB	1.41	13.5	N/A	2.6×10^{-3}	1.84×10^{4}	11
	H_2O_2	0.11	28.5		5.5×10^{-3}	5×10^{6}	
OsNHs	TMB	0.12	7.7	2.77×10^{-6}	2.78×10^{4}	2.31×10^{5}	This
	H_2O_2	8.30	16		5.78×10^{4}	6.96×10^{3}	work

246 **HRP**-horseradish peroxidase; **hNS**-hollow nanostructures; **NFs**-nanoflowers; **MFs**-microflowers;

247 **Pt10-LP NCs**-Lily polysaccharide stabilized platinum nanoclusters.

248

249

250

Table S2 Comparison between different methods used for the determination of FA.

Method	Materials used	LOD (μg·mL^{-1})	Linear range (μg·mL^{-1})	Analysis time (min)	Ref.
HPLC	N.S.	0.03	2.9-8.7	＞30 min	12
LC/MS/MS	N.S.	0.02	0.02-293	＞30 min	13
HPLC/ESI-MS	N.S.	9×10^{-3}	0.01-50	＞30 min	14
Uv-sp	N.S.	9.3×10^{-3}	1-17.5	＞30 min	15
ELISA	HRP	2×10^{-3}	4.8×10^{-3}-8.17×10^{-2}	300min	2
FLISA	AgInS/ZnS	1×10^{-4}	2×10^{-3}-0.047	250min	16
QDs-LFIA	QDs	0.5	0.9-6.7	20min	16
HRP-ELISA	HRP	12.3×10^{-3}	0.036-1.68	300min	This work
OsNHs-ELISA	OsNHs	4.03×10^{-3}	9.4×10^{-3}-0.17	250min	This work
AuNPs-LFIA	AuNPs	N.S.	N.S.	5 min	This work
OsNHs-LFIA	OsNHs	N.S.	N.S.	5 min	This work

N.S.=not state.

Table S3 Elaborate information of Mobile phase composition and gradient elution

Time（min）	%A	%B
0	90	10
2	90	10
3	10	90
5	10	90
5.1	90	10
7	90	10

Solvent A：0.1% Formic acid aqueous solution; Solvent B：Methanol.

Flow-rate：0.3 $mL \cdot min^{-1}$;

Temperature of column oven: 40℃；

Sample solution volume 2 μL.

Table S4 Mass spectrometry parameters setting

MS parameters	SV
Ionization mode	H-ESI +
Spray Voltage (V)：	3500
Vaporizer Temperature (℃)	350
Capillary Temperature (℃)	320
Sheath Gas (Arb)	35
AUX Gas (Arb)	10
Sweep Gas (Arb)	0

References

1. H. P. Zhu, T. T. Liu, B. Liu, H. L. Yin, X. L. Li, L. Wang and S. Wang, *Chinese Chem Lett*, 2010, **21**, 1049-1052.
2. T. Zhang, H. Xue, B. Zhang, Y. Zhang, P. Song, X. Tian, Y. Xing, P. Wang, M. Meng and R. Xi, *J Sci Food Agric*, 2012, **92**, 2297-2304.
3. Q. He, Y. Chen, D. Shen, X. Cui, C. Zhang, H. Yang, W. Zhong, S. A. Eremin, Y. Fang and S. Zhao, *Talanta*, 2019, **195**, 655-661.
4. P. Cai, R. Wang, S. Ling and S. Wang, *Food Chem*, 2021, **360**, 130021.
5. L. Gao, J. Zhuang, L. Nie, J. Zhang, Y. Zhang, N. Gu, T. Wang, J. Feng, D. Yang, S. Perrett and X. Yan, *Nat Nanotechnol*, 2007, **2**, 577-583.
6. J. Dong, L. Song, J. J. Yin, W. He, Y. Wu, N. Gu and Y. Zhang, *ACS Appl Mater Interfaces*, 2014, **6**, 1959-1970.
7. N. V. Long, M. Ohtaki, M. Uchida, R. Jalem, H. Hirata, N. D. Chien and M. Nogami, *J Colloid Interface Sci*, 2011, **359**, 339-350.
8. S. B. He, L. Yang, P. Balasubramanian, S. J. Li, H. P. Peng, Y. Kuang, H. H. Deng and W. Chen, *Journal of Materials Chemistry A*, 2020, **8**, 25226-25234.
9. G. J. Cao, X. Jiang, H. Zhang, T. R. Croley and J. J. Yin, *Rsc Adv*, 2017, **7**, 52210-52217.
10. L. Y. Fan, X. B. Ji, G. Q. Lin, K. Liu, S. F. Chen, G. L. Ma, W. L. Xue, X. Y. Zhang and L. G. Wang, *Microchemical Journal*, 2021, **166**, 106202.
11. W. C. Zhang, X. H. Niu, S. C. Meng, X. Li, Y. F. He, J. M. Pan, F. X. Qiu, H. L. Zhao and M. B. Lan, *Sensor Actuat B-Chem*, 2018, **273**, 400-407.
12. P. Jin, L. Xia, Z. Li, N. Che, D. Zou and X. Hu, *J Pharm Biomed Anal*, 2012, **70**, 151-157.
13. B. C. Nelson, K. E. Sharpless and L. C. Sander, *J Chromatogr A*, 2006, **1135**, 203-211.
14. Z. Chen, B. Chen and S. Z. Yao, *Analytica Chimica Acta*, 2006, **569**, 169-175.
15. M. K. Off, A. E. Steindal, A. C. Porojnicu, A. Juzeniene, A. Vorobey, A. Johnsson and J. Moan, *J Photochem Photobiol B*, 2005, **80**, 47-55.
16. Y. He, S. Wang and J. P. Wang, *Food Anal. Meth.*, 2021, **14**, 1637-1644.